# Temperature-Adaptive Driving Waveform With Multiscan High Voltages for Stable Address Discharge in AC Plasma Display Panel

Soo-Kwan Jang, Choon-Sang Park, Heung-Sik Tae, *Senior Member, IEEE*, Bhum Jae Shin, *Member, IEEE*, and Jeong Hyun Seo

***Abstract*—The discharge characteristics, particularly the address discharge characteristics, were examined relative to an ambient temperature from −5 °C to +65 °C in an ac plasma display panel. As the ambient temperature increased, the statistical delay time decreased due to an increase in the exoelectron emission from the MgO surface by thermal activation. In contrast, the formative delay time increased due to an increase in the wall voltage variation during an address period. It was also found that the wall voltage variation during an address period depended on the level of the scan high voltage. Therefore, a temperature-adaptive driving waveform with multiscan high voltages is proposed to produce a stable address discharge irrespective of a variable ambient temperature.**

***Index Terms*—Ambient temperature, exoelectron emission, stable address discharge, temperature-adaptive driving waveform, wall voltage variation.**

## I. Introduction

THE AMBIENT temperature is an important factor affecting stable discharge in plasma display panel (PDP) cells, as the discharge characteristics vary depending on the ambient temperature. In particular, the address discharge characteristics are strongly dependent on the ambient temperature, where misfiring problems are caused at a high ambient temperature [1], [2]. While this phenomenon would appear to be closely related to the exoelectron emission affected by the ambient temperature [3]–[5], the temperature dependency of the address discharge characteristics in relation to the MgO surface phenomenon is still not well understood.

Accordingly, this paper investigated the address discharge characteristics relative to the ambient temperature to explain the temperature dependency of the address discharge characteristics. As a result, it was found that the driving parameters related to the ambient temperature, including the number of sustain pulses and the voltage level applied to the scan electrode during the address period, were also important factors affecting the address discharge characteristics. Therefore, based on these experimental observations, a temperature-adaptive driving waveform with multiscan high voltages is proposed to produce a stable address discharge irrespective of a variable ambient temperature.

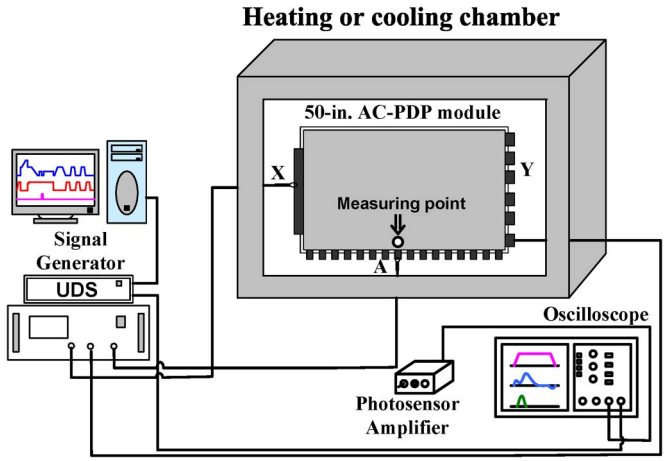


Fig. 1. Schematic of the experimental setup for overall heating of 50-in test panel with three electrodes inside heating (or cooling) chamber, where X is common electrode, Y is scan electrode, and A is address electrode.

## II. Experimental Setup

Fig. 1 shows a schematic of the experimental setup used for the measurements. A 50-in test panel with a working gas pressure of 420 torr was employed in this paper, and its structure and dimensions were exactly the same as those of a conventional 50-in full-HD ac PDP with a box-type barrier rib. The gas mixtures used were He (50%)–Ne–Xe (11%). The detailed panel specifications are listed in Table I. As shown in Fig. 1, the ambient temperature of the test panel was varied from −5 °C to +65 °C by heating or cooling the heating (or cooling) chamber. To avoid the ambient temperature from influencing the electronic circuits, all electronic equipment were positioned outside the heating (or cooling) chamber. Plus, since the address discharges are aggravated in the lower part of the panel when carrying out the line-by-line scan in the address-display-separated

Manuscript received August 12, 2010; revised July 15, 2010; accepted July 27, 2010. Date of publication September 2, 2010; date of current version November 5, 2010. This work was supported in part by the IT&D program of MKE/KEIT (KI002199, Development of Eco-friendly 50″ Quadro Full HD PDP Technology) and in part by Brain Korea 21 (BK21). The review of this paper was arranged by Editor J. Kanicki.

S.-K. Jang, C.-S. Park, and H.-S. Tae are with the School of Electronics Engineering, College of IT, Kyungpook National University, Daegu 702-701, Korea.

B. J. Shin is with the Department of Electronics Engineering, Sejong University, Seoul 143-747, Korea.

J. H. Seo is with the Department of Electronics Engineering, University of Incheon, Incheon 402-751, Korea.

Color versions of one or more of the figures in this paper are available online at http://ieeexplore.ieee.org.

Digital Object Identifier 10.1109/TED.2010.2066111

TABLE I
SPECIFICATIONS OF 50-in TEST PANEL EMPLOYED IN THIS PAPER

| | |
|---|---|
| Pixel pitch | 192 μm x 576 μm |
| Dielectric layer thickness | 30 μm |
| Rib height | 120 μm |
| Gas mixture | He (50 %) – Ne – Xe (11 %) |
| Pressure | 420 Torr |
| ITO width | 200 μm |
| ITO gap | 70 μm |
| Address electrode width | 90 μm |

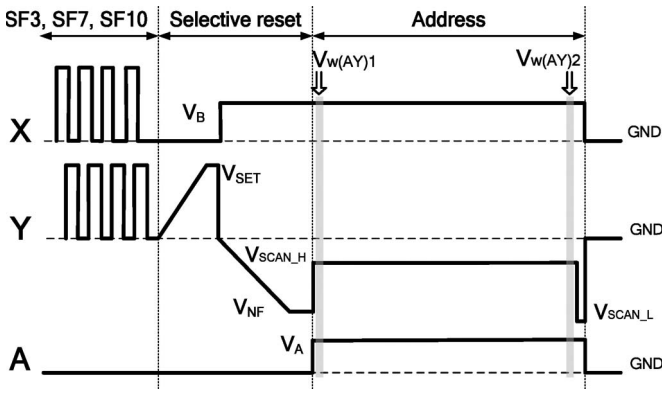


Fig. 2. Driving waveform employed to measure wall voltage variation during address period.

TABLE II
VARIOUS VOLTAGE LEVELS EMPLOYED IN DRIVING WAVEFORM IN FIG. 2

| | Voltage [V] |
|---|---|
| $V_B$ | 110 |
| $V_{SET}$ | 200 |
| $V_{NF}$ | -160 |
| $V_A$ | 65 |
| $V_{SCAN\,H}$ | -70 |
| $V_{SCAN\,L}$ | -180 |

driving scheme, the address discharge characteristics of the last scan line in the lower part of the panel were measured under various ambient temperatures, as shown in Fig. 1 [6].

## III. EFFECT OF AMBIENT TEMPERATURE AND SUSTAIN DISCHARGE ON ADDRESS DISCHARGE

Fig. 2 shows the driving waveform employed to measure the address discharge characteristics. The applied sustain pulses were ten pairs for the lower subfield (SF 3), 50 pairs for the middle subfield (SF 7), and 100 pairs for the upper subfield (SF 10). The width of the address pulses was 1.25 $\mu$s, making the address periods 1350 $\mu$s for 1080 scan lines (i.e., full-white pattern). In addition, the applied voltage levels in Fig. 2 are listed in Table II.

Fig. 3 shows the formative delay time $(T_f)$ and the statistical delay time $(T_s)$ measured at SF 3 when varying the ambient temperature from $-5$ °C to $+65$ °C. As the ambient temperature increased, the statistical delay time $(T_s)$ decreased, whereas the formative delay time $(T_f)$ increased. It is already known that the statistical delay time $T_s$ is influenced by the number

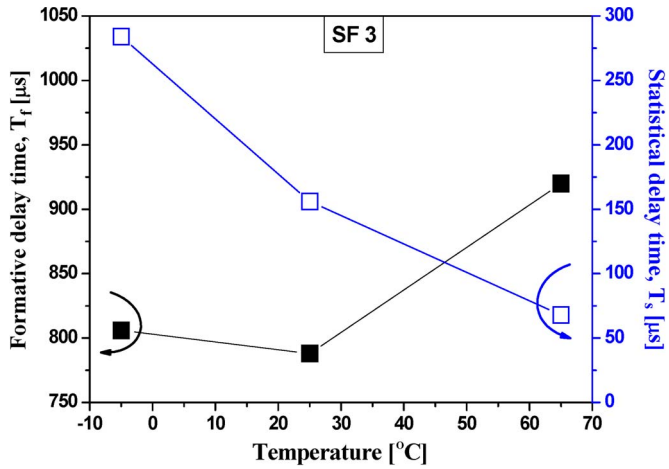


Fig. 3. Address discharge delay times $T_f$ and $T_s$ measured in SF 3 when varying the ambient temperature from $-5$ °C to $+65$ °C.

TABLE III
PARAMETER VALUES USED IN THIS CALCULATION

| Parameters | Value |
|---|---|
| N (trap conc.) | $10^{19}$ |
| $n_0$(initial trapped electron conc.) | $10^{16}$ |
| $A_m/A_n$ | 1.0 |
| K (temperature) | 298 |
| υ (Debye freq.) | $10^{13}$ |
| k (Boltzmann constant) | $1.6 \times 10^{-19}$ |
| $E_t$(trap energy level) | 0.4 |

of electrons supplied to the discharge space, that is, priming particles, as in the following equation [7]:

$$T_s = \frac{1}{n_0 P_s} \tag{1}$$

where $n_0$ is the number of seed electrons, and $P_s$ is the probability of an avalanche.

Thus, the statistical delay time is inversely proportional to the concentration of seed electrons. The seed electrons are supplied by the exoelectron emission from the MgO surface during an address period [3]–[5]. The exoelectron current $I(t)$ can be described using the following equation [8]–[10]:

$$I(t) = \frac{k_3 k_2 n_0^2}{(1 + k_2 n_0 t)^2}$$
$$k_2 = \frac{A_m \upsilon \exp\left(-\frac{E_t}{RT}\right)}{N A_n} \tag{2}$$

where $k_3$ is the probability of the constant emission of exited electrons, $n_o$ is the initial trapped electron concentration, $\upsilon$ is the Debye frequency, $E_t$ is the energy level of the electron trap, $R$ is the gas constant, $T$ is the temperature, $N$ is the number of donor sites, and $A_n$ is the retrapping reaction rate constant.

Using (2), the exoelectron currents were calculated as a function of the ambient temperature using the parameter values listed in Table III. As shown in Fig. 4, as the ambient temperature increased, the exoelectron current also increased. Consequently, the statistical delay time was observed to decrease in proportion to the ambient temperature. In contrast, the formative delay time $(T_f)$ was observed to increase in

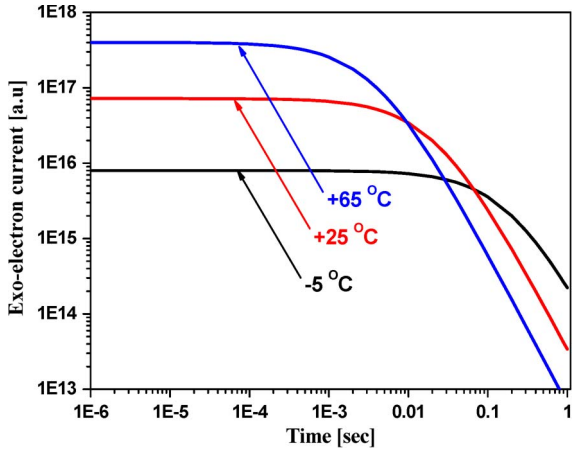


Fig. 4. Exoelectron currents calculated using (2) in SF 3 when varying the ambient temperature from −5 °C to +65 °C.

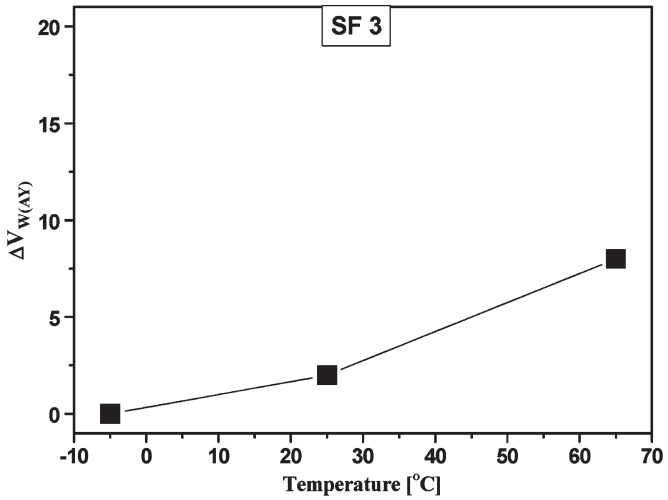


Fig. 5. Wall voltage variation measured during address period relative to ambient temperature at SF 3.

proportion to the ambient temperature, as shown in Fig. 3. It has also been established that the formative delay time $(T_f)$ can be described using the following equation [11]:

$$T_f = \frac{d}{EK_+} + \frac{d}{EK_e} \approx \frac{d}{EK_+} \tag{3}$$

where $d$ is the gap length, $E$ is the electric field strength, $K_+$ is the ion mobility, and $K_e$ is the electron mobility.

As shown in (3), the formative delay time is inversely proportional to the electric field intensity between the A and Y electrodes, which infers that the increase in the formative delay time when increasing the ambient temperature can be attributed to the decrease in the electric field intensity.

Fig. 5 shows the wall voltage variation, defined by $V_{w(\mathrm{AY})1} - V_{w(\mathrm{AY})2}$ and indicated in Fig. 2, which was measured using the $V_t$ closed curve technique when varying the ambient temperature from −5 °C to +65 °C [12]. As expected, the increase in the formative time was surely related to the wall voltage variation, which decreased the electric field between the A–Y electrodes when increasing the ambient temperature.

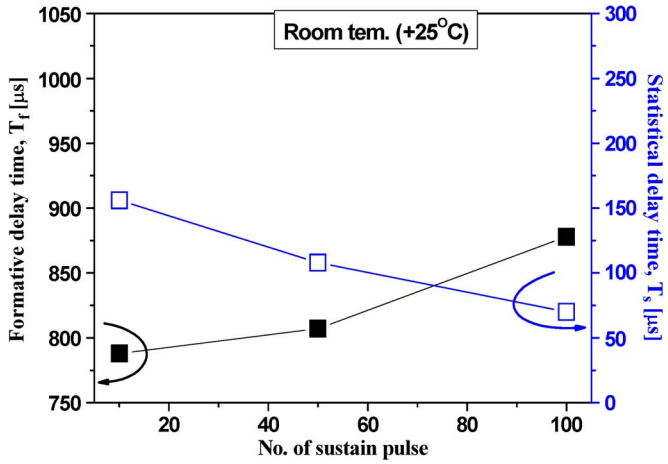


Fig. 6. Address discharge delay times $T_f$ and $T_s$ measured at room temperature (+25 °C) when varying the number of applied sustain pulses from 10 to 100.

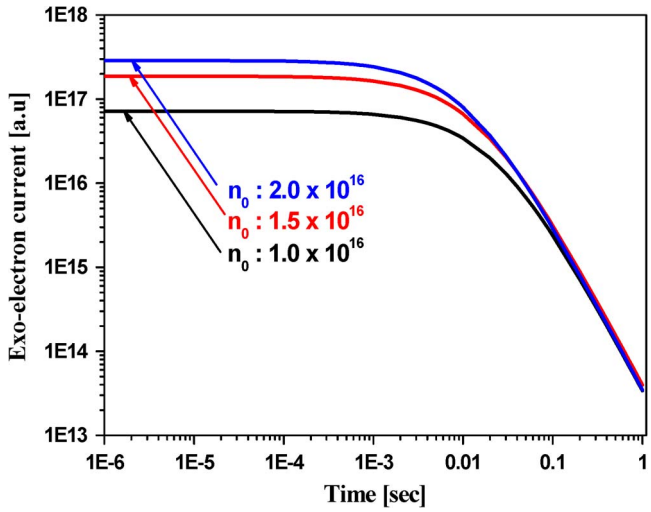


Fig. 7. Exoelectron currents calculated using (2) at room temperature (+25 °C) when varying the initial trapped electron concentration $n_o$ in proportion to number of applied sustain pulses.

As the misfiring of a small number of cells is often observed at a high ambient temperature, particularly in the upper subfield condition [1], the number of sustain pulses may be another factor affecting the address discharge characteristics relative to the ambient temperature.

Fig. 6 shows the address discharge delay times according to the number of applied sustain pulses at room temperature. Fig. 7 shows the exoelectron currents calculated using (2) at room temperature when varying the initial trapped electron concentration $n_o$ in proportion to the number of applied sustain pulses. The initial trapped electron concentration $n_o$ is known to be increased with an increase in the applied sustain pulse number [13]. As shown in Fig. 6, when the number of applied sustain pulses increased, the statistical delay time decreased. Since the electrons caught in the trap level of the MgO surface likely increased in proportion to the number of sustain discharges, this produced an increase in the exoelectron current, as shown in Fig. 7. The increase in the exoelectron emission from the MgO

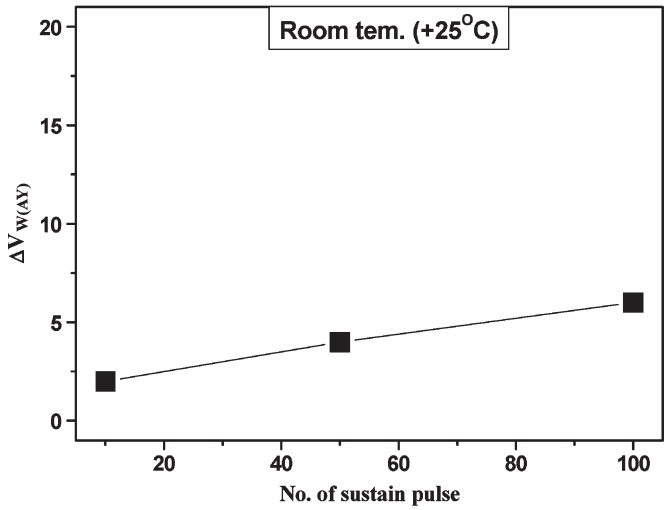


Fig. 8. Wall voltage variation measured during address period relative to the number of applied sustain pulses at room temperature (+25 °C).

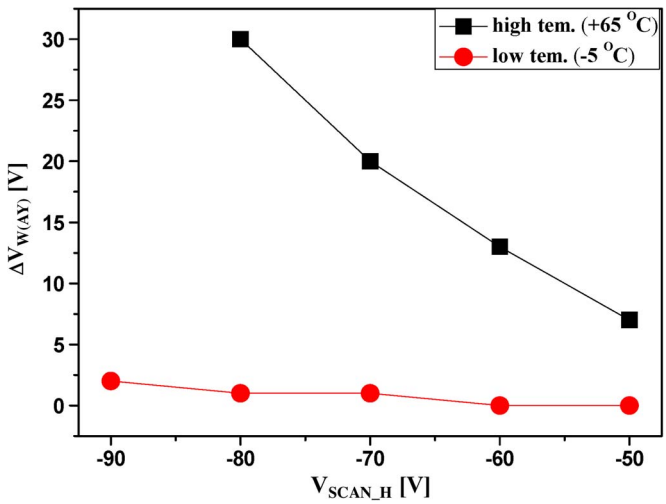


Fig. 9. Influence of scan high voltage ($V_{\mathrm{SCAN\_H}}$) and ambient temperature on wall voltage variation during address period at SF 10.

surface due to the increase in the sustain pulse number resulted in reducing the statistical delay time.

However, the formative delay time increased as the wall voltage variation increased when increasing the number of applied sustains pulses, as shown in Fig. 8. In Fig. 8, the wall voltage variation occurred depending on the number of applied sustain pulses during an address period. However, the wall voltages $V_{w(\mathrm{AY})1}$ measured after the reset discharge showed no difference irrespective of the number of applied sustain pulses, implying that the variations in the electrons caught in the trap level of the MgO surface according to the number of applied sustain pulses did not affect the formation of the wall charges during the reset period. Finally, the wall voltage variation during the address period was confirmed to be related to the increase in the exoelectron emission caused by the increase in the number of applied sustain pulses. Consequently, the statistical delay time was found to decrease, whereas the formative delay time increased when increasing the number of applied sustain pulses.

Fig. 9 shows the influence of the scan high voltage ($V_{\mathrm{SCAN\_H}}$) and the ambient temperature on the wall voltage variation during an address period in the upper subfield (SF 10). At an ambient temperature of +65 °C, the wall voltage variation increased from 7 to 30 V when $|V_{\mathrm{SCAN\_H}}|$ was increased from 50 to 80 V. However, at an ambient temperature of −5 °C, the wall voltage variation slightly changed when $|V_{\mathrm{SCAN\_H}}|$ was increased from 50 to 80 V. As described in Figs. 4 and 7, the high temperature condition at SF 10 emitted greater exoelectrons in the discharge space. In this case, the wall voltage variation increased depending on the electric field intensity between the A–Y electrodes induced the voltage difference between $V_A$ and $V_{\mathrm{SCAN\_H}}$ during an address period. In other words, under the high exoelectron emission condition, the wall voltage was varied considerably according to the electric field intensity applied between the A–Y electrodes. On the other hand, at a low temperature condition emitting lesser exoelectrons into discharge space, the wall voltage was little influenced by the variation in the electric field intensity. Therefore, these results

TABLE IV
MULTISCAN HIGH VOLTAGES RELATIVE TO SUBFIELD AND AMBIENT TEMPERATURE IN MODIFIED DRIVING WAVEFORM

| Multi scan high voltages ($V_{\mathrm{SCAN\_H}}$) | | |
|---|---|---|
| | Lower sub-field | Upper sub-field |
| -5 °C | -90 V | -70 V |
| +25 °C | -70 V | -70 V |
| +65 °C | -70 V | -50 V |

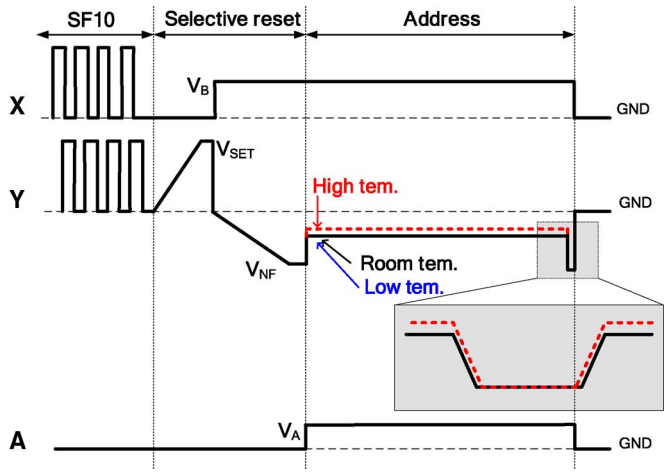


Fig. 10. Proposed driving waveform with multiscan high voltages in the upper subfield (SF 10), where the scan high voltage is varied according to ambient temperature: $V_{\mathrm{SCAN\_H}}$ is −50 V at +65 °C, and −70 V at +25 °C and −5 °C.

indicate that the wall voltage variation phenomenon is closely related to the electric field intensity in the discharge space as well as the ambient temperature, implying that the exoelectrons emitted from the MgO surface by thermal activation at a high ambient temperature might be amplified in the discharge space due to the high electric field intensity, thereby resulting in causing a wall voltage variation due to the recharging phenomenon. However, this phenomenon needs to be studied further [14].

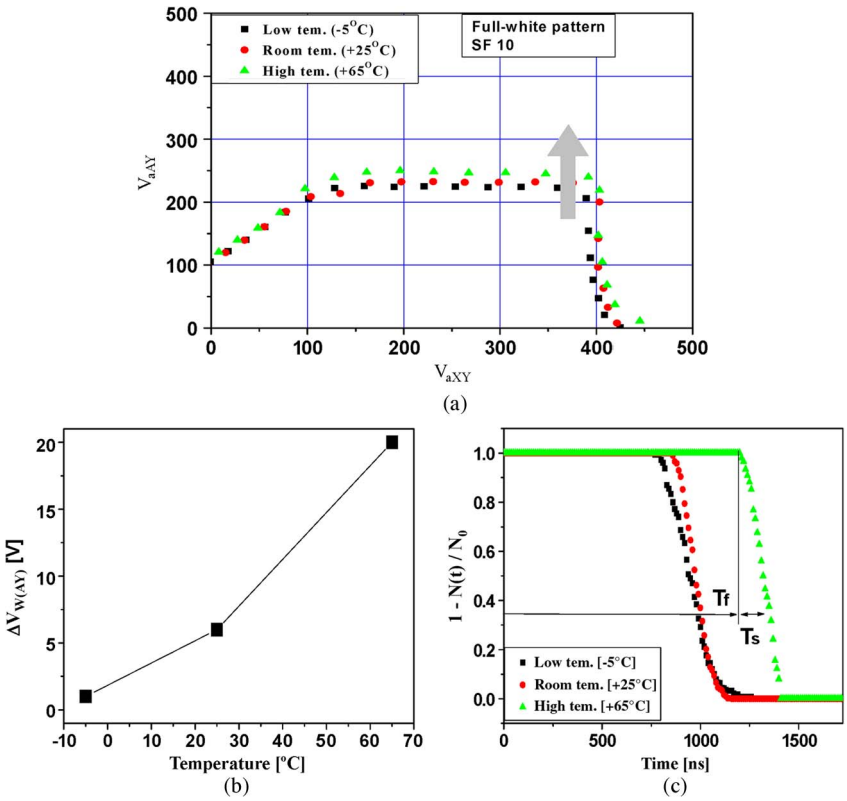


Fig. 11. $V_t$ closed curve and address delay time measured in the upper subfield when applying the conventional driving waveform.

## IV. Modified Driving Waveform With Multiscan High Voltages for Stable Address Discharge Under Variable Temperature

As previously described, the wall voltage variation is directly related to the ambient temperature and the driving parameters related to the ambient temperature, such as the number of the sustain pulses and $V_{\mathrm{SCAN\_H}}$ level. That is, the wall voltage variation increases both when increasing the ambient temperature and when increasing the number of sustain pulses. It should be noted that the $|V_{\mathrm{SCAN\_H}}|$ level is an important parameter causing a wall voltage variation during the address period, as shown in Fig. 9. Thus, to maintain a stable address discharge under a variable ambient temperature, the conventional driving waveform needs to be modified to compensate the wall voltage variation relative to the ambient temperature. Therefore, a new driving waveform with a variable scan high voltage $(V_{\mathrm{SCAN\_H}})$ adaptive to the ambient temperature is proposed. The basic idea of the proposed driving waveform is to apply an adaptive $|V_{\mathrm{SCAN\_H}}|$ according to the ambient temperature and subfield conditions to minimize the wall voltage variation, thereby producing a stable address discharge.

The adaptive scan high voltages according to the ambient temperature and subfield conditions are given in Table IV.

Fig. 10 shows the proposed driving waveform in the upper subfield (SF 10), where the scan high voltage is varied according to the ambient temperature, as shown in Table IV. Under this condition, $-50$ V is selected for $V_{\mathrm{SCAN\_H}}$ to minimize the wall voltage variation at high ambient temperature $(+65\ ^{\circ}\mathrm{C})$.

Fig. 11(a)–(c) shows the $V_t$ closed curve, the wall voltage variation, and the Laue plot of the address delay time measured in the upper subfield when applying the conventional driving waveform. The Laue plot in Fig. 11(c) can be described using the following equation [11]:

$$\begin{aligned}&\text{Probability of nondischarge } (P)\\ &\quad = \exp\left[-(t-T_f)/T_s\right] \quad (t \geq T_f)\\ &\quad = 1 \qquad (0 \leq t \leq T_f)\end{aligned} \tag{4}$$

where $T_f$ is the formative delay time, and $T_s$ is the statistical delay time.

In (4), $P = 1$ means that no address discharge was completed, whereas $P = 0$ means that every address discharge was completed. As shown in Fig. 11(a), as the ambient temperature increased, the $V_t$ closed curves measured particularly in the first quadrant were moved to the upward direction, implying that the shift of the $V_t$ closed curve to the upward direction meant the reduction in the wall voltage between the A–Y electrodes due to a rise in the ambient temperature. Fig. 11(b) shows the wall voltage variation between the A–Y electrodes $(\Delta V_{w(\mathrm{AY})} = V_{w\mathrm{A}} - V_{w\mathrm{Y}})$ calculated from the measured $V_t$ closed curves in Fig. 11(a). The wall voltage variations between the A–Y electrodes were observed to be almost the same at room temperature $(+25\ ^{\circ}\mathrm{C})$ and at low temperature $(-5\ ^{\circ}\mathrm{C})$. However, the wall voltage variation sharply increased at a higher ambient temperature. As a result, as shown in Fig. 11(c), the formative delay time increased at high ambient temperature due to the increase in the wall voltage variation.

Fig. 12 shows the $V_t$ closed curve, the wall voltage variation, and the Laue plot of the address delay time measured in the upper subfield when applying the proposed modified driving

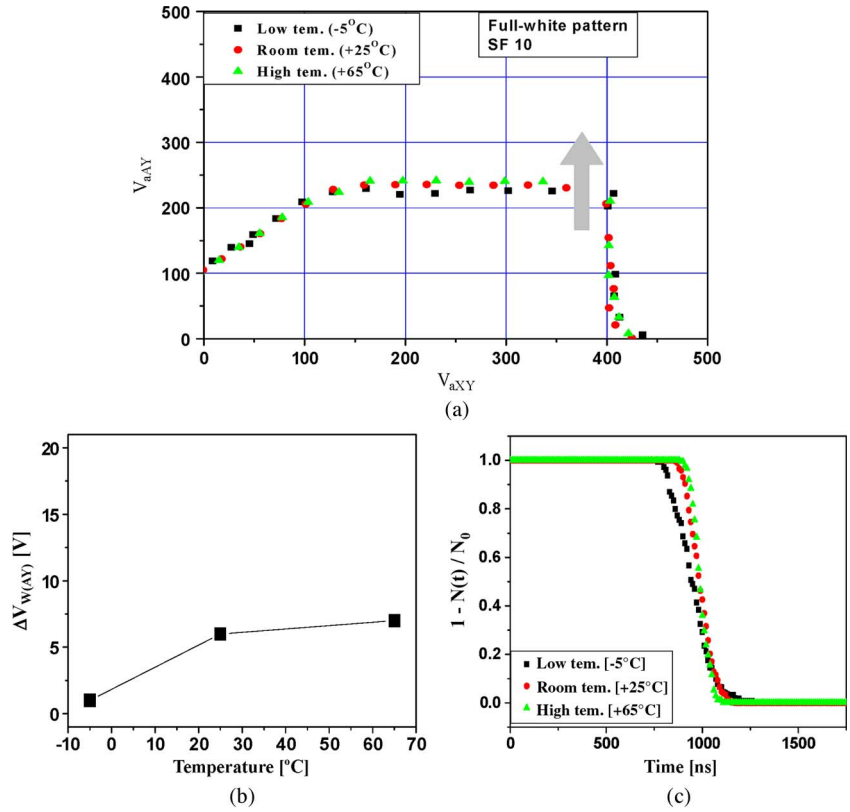


Fig. 12. $V_t$ closed curve and address delay time measured in the upper subfield when applying modified driving waveform.

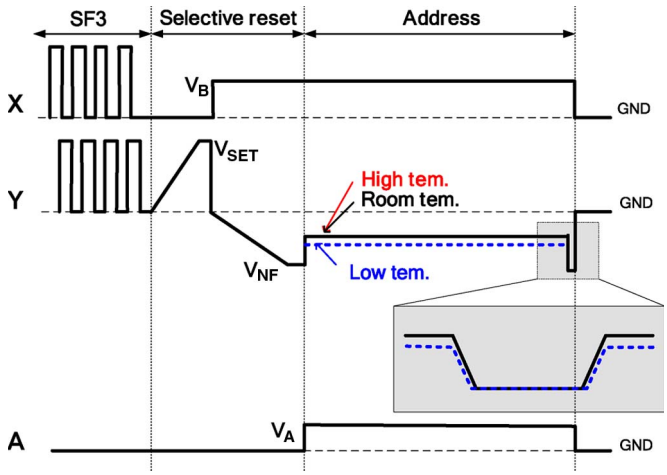


Fig. 13. Proposed driving waveform with multiscan high voltages in the lower subfield (SF 3), where the scan high voltage is varied according to ambient temperature: $V_{\mathrm{SCH\_H}}$ is $-90$ V at $-5$ °C and $-70$ V at $+25$ °C and $+65$ °C.

waveform in Fig. 10. As shown in Fig. 12(b), the wall voltage variations between the A–Y electrodes were minimized under a variable ambient temperature. As a result, the formative delay time was noticeably reduced at high temperature $(+65\ ^{\circ}\mathrm{C})$, thereby allowing a stable address discharge under a variable ambient temperature.

Fig. 13 shows the proposed driving waveform with multiscan high voltages in the lower subfield (SF 3), where the scan high voltage was varied according to the ambient temperature, as shown in Table III. Under this condition, $-90$ V was selected for $V_{\mathrm{SCAN\_H}}$ at a low ambient temperature $(-5\ ^{\circ}\mathrm{C})$, thereby reducing the switching voltage applied to the Y electrode for the address operation when compared with the conventional driving scheme.

Figs. 14 and 15 show the $V_t$ closed curve, the wall voltage variation, and the Laue plot of the address delay time measured in the lower subfield when applying the conventional and modified driving waveforms, respectively. When comparing Figs. 14(b) and 15(b), the wall voltage variations between the A–Y electrodes were almost the same, irrespective of the ambient temperature; however, the address delay time at low temperature $(-5\ ^{\circ}\mathrm{C})$ increased when applying the conventional driving waveform, whereas the statistical delay time increased due to the poor priming condition [8]. In contrast, when applying the modified driving waveform, the difference in address delay time caused by the variable ambient temperature was minimized, as shown in Fig. 15(c), based on reducing the falling time of the scan pulse by applying the maximum scan high voltage $(|V_{\mathrm{SCAN\_H}}| = |-90\ \mathrm{V}|)$.

## V. Conclusion

Due to its importance for discharge stability, this paper investigated the relation between the address discharge characteristics and the ambient temperature. Experiments showed that when increasing the ambient temperature, the statistical delay time was decreased due to an increase in the exoelectron emission current, whereas the formative delay time was increased due to an increase in the wall voltage variation between the A–Y electrodes. It should be noted that the wall voltage variation, which affects the address discharge, was also

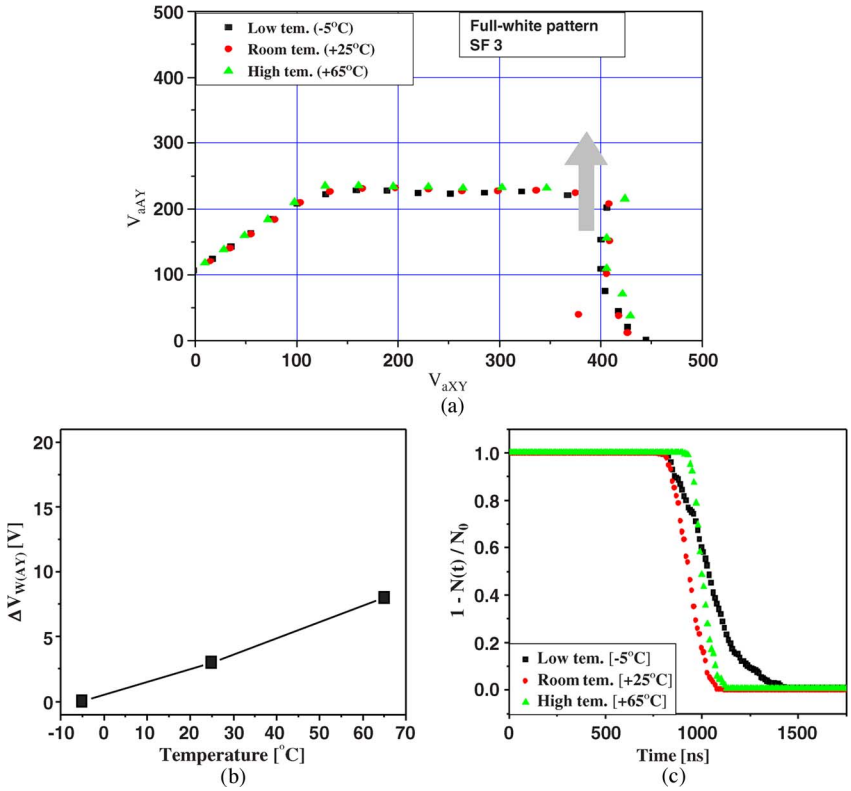


Fig. 14. $V_t$ closed curve and address delay time measured in the lower subfield when applying conventional driving waveform.

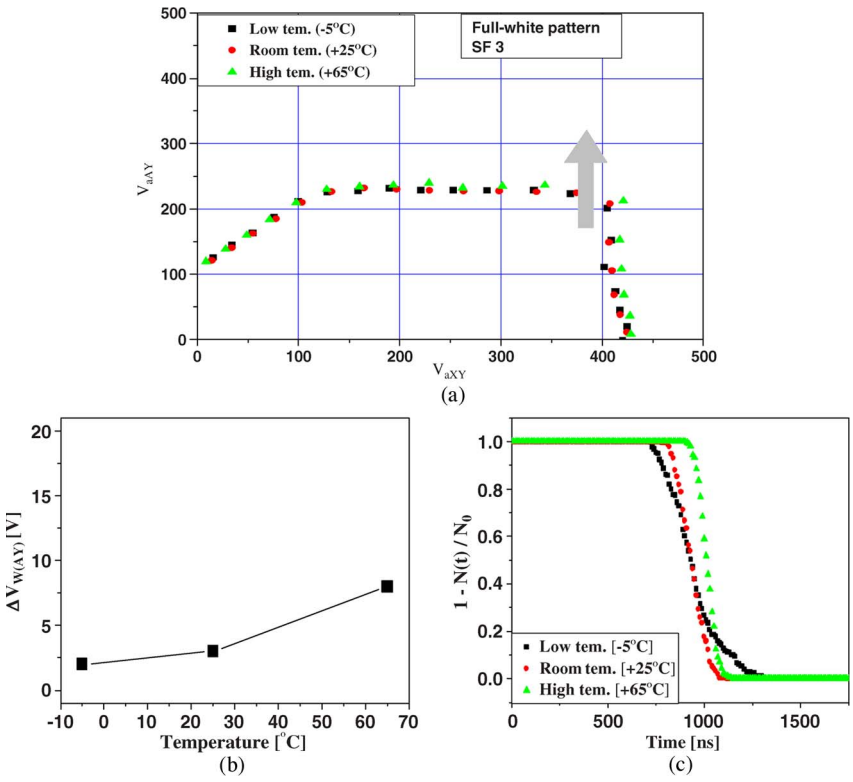


Fig. 15. $V_t$ closed curve and address delay time measured in the lower subfield when applying modified driving waveform.

influenced by the driving parameters, such as the number of sustain pulses and $V_{\mathrm{SCAN\_H}}$ level, related to the ambient temperature. Experimental results showed that a modified driving waveform with multiscan high voltages $(V_{\mathrm{SCAN\_H}})$ adaptive to the ambient temperature and subfield conditions was able to minimize the wall voltage variation. Consequently, the modified driving waveform was demonstrated to produce a stable address discharge under a variable ambient temperature.

## REFERENCES


[1] J.-H. Ryu, J.-Y. Choi, H.-J. Lee, D.-H. Kim, H. H. Lee, and C.-H. Park, "Experimental observation and modified driving method to improve the high-temperature misfiring in AC PDP," *IEEE Trans. Electron Devices*, vol. 52, no. 12, pp. 2026–2032, Dec. 2004.

[2] S.-K. Jang, H.-S. Tae, S.-B. Kim, E.-Y. Jung, K.-J. Suh, J.-C. Ahn, E.-G. Heo, B.-H. Lee, and K.-S. Lee, "Observation on discharge characteristics under variable panel temperature and modified ramp-reset waveform robust for variable panel temperature," in *Proc. IDW Dig.*, 2005, pp. 1473–1476.

[3] Q. F. Yan, N. Kosugi, Y. Oe, H. Tachibana, and L. F. Weber, "Analysis of priming source for addressing discharge of AC PDP," in *Proc. IDW Dig.*, 2006, pp. 359–362.

[4] T. Okada, T. Furutani, and T. Yoshioka, "Decay kinetics of electron emission from MgO films in AC plasma display panels," *Appl. Phys. Express*, vol. 1, no. 9, p. 091 203, Sep. 2008.

[5] C.-R. Hong, S.-H. Yoon, and Y.-S. Kim, "Effects of EXO-electron emission from MgO thin film on statistical delay of glow discharge of AC-PDP," *Thin Solid Films*, vol. 517, no. 14, pp. 4170–4173, May 2009.

[6] B.-T. Choi, H. D. Park, and H.-S. Tae, "Effect of address-on-time on wall voltage variation during address-period in AC-plasma display," *IEICE Trans. Electron.*, vol. E92-C, no. 11, pp. 1347–1352, Nov. 2009.

[7] L. B. Loeb, "Statistical factors in spark discharge mechanisms," *Rev. Mod. Phys.*, vol. 20, no. 1, pp. 151–160, Jan. 1948.

[8] L. Oster, V. Yaskolko, and J. Haddad, "Classification of exoelectron emission mechanisms," *Phys. Stat. Sol. (A)*, vol. 174, no. 2, pp. 431–439, 1999.

[9] M. Molotskii, M. Naich, and G. Rosenman, "Auger mechanism of exoelectron emission in dielectrics with high electron affinity," *J. Appl. Phys.*, vol. 94, no. 7, pp. 4652–4657, Oct. 2003.

[10] S.-H. Yoon, S.-G. Ahn, and Y.-S. Kim, "Control of temperature dependency of EXO-electron emission behavior for MgO film of AC-PDPs," in *Proc. SID Dig.*, 2009, pp. 353–355.

[11] N. Uemura, Y. Yajima, M. Shibata, Y. Kawanami, and F. Namiki, "Improvement of the speed of address discharge in Ne-Xe-He discharge gases for ACPDPs," in *Proc. SID Dig.*, 2003, pp. 1469–1472.

[12] H.-S. Tae, S.-K. Jang, K.-D. Cho, and K.-H. Park, "High-speed driving method using bipolar scan waveform in AC plasma display panel," *IEEE Trans. Electron Devices*, vol. 53, no. 2, pp. 196–204, Feb. 2006.

[13] S.-H. Yoon, H.-W. Ryu, C.-R. Hong, D.-H. Kim, J.-J. Ko, and Y.-S. Kim, "Measurement of exo-electron emission from MgO thin film of AC-PDP," in *Proc. SID Dig.*, 2008, pp. 287–290.

[14] S.-K. Jang, C.-S. Park, H.-S. Tae, B. J. Shin, J. H. Seo, and E.-Y. Jung, "Effect of Xe content on wall voltage-variation during address-period in AC plasma-display panel," *J. Soc. Inf. Displ.*, vol. 18, no. 18, pp. 614–649, Aug. 2010.


**Soo-Kwan Jang** received the B.S., M.S., and Ph.D. degrees in electronic and electrical engineering from Kyungpook National University, Daegu, Korea, in 2003, 2005, and 2010, respectively.

Since 2010, he has been a Postdoctoral Fellow with the School of Electrical Engineering and Computer Science, Kyungpook National University. His current research interests include plasma physics and driving waveform of plasma display panels (PDPs).

**Choon-Sang Park** received the M.S. and Ph.D. degrees in electronic and electrical engineering from Kyungpook National University, Daegu, Korea, in 2006 and 2010, respectively.

Since 2010, he has been a Postdoctoral Fellow with the School of Electrical Engineering and Computer Science, Kyungpook National University. His current research interests include microdischarge physics, MgO thin film, driving waveform of plasma display panels (PDPs), and surface analysis for new material.

**Heung-Sik Tae** (M'00–SM'05) received the B.S., M.S., and Ph.D. degrees in electrical engineering from Seoul National University, Seoul, Korea, in 1986, 1988, and 1994, respectively.

Since 1995, he has been a Professor with the School of Electronics Engineering, College of IT, Kyungpook National University, Daegu, Korea. His research interests include the optical characterization and driving waveform of plasma display panels (PDPs).

Dr. Tae is a member of the Society for Information Display (SID). He has been serving as an Editor for the IEEE TRANSACTIONS ON ELECTRON DEVICES section on display technology since 2005.

**Bhum Jae Shin** (M'03) received the B.S., M.S., and Ph.D. degrees in plasma engineering from Seoul National University, Seoul, Korea, in 1990, 1992, and 1997, respectively.

From 1997 to 2000, he was a Senior Researcher with the PDP team, Samsung SDI, Cheonan, Korea, where worked on the development of PDPs. From 2000 to 2001, he was a Visiting Researcher with the Physics Department, Stevens Institute of Technology, Hoboken, NJ, where he worked on capillary discharges. In 2003, he joined the Department of Electronics Engineering, Sejong University, Seoul, where he is currently an Assistant Professor. His research interests include high-efficiency cell structures and the driving circuit of plasma display panels (PDPs).

**Jeong Hyun Seo** received the B.S., M.S., and Ph.D. degrees in plasma engineering from Seoul National University, Seoul, Korea, in 1993, 1995, and 2000, respectively.

He was with Plasma Display Panel (PDP) Division, Samsung SDI, Cheonan, Korea, from 2000 to 2002, where his work focused on the design of driving pulse in ac PDP. Since September 1, 2002, he has been a Professor with the Department of Electronics Engineering, University of Incheon, Incheon, Korea. His research is currently focused on the high-efficiency PDP cell structure, driving method, and numerical modeling in PDP.

Dr. Seo is a member of the Society for Information Display (SID) and the Korean Information Display Society.